

# Recent Negative Ion Source Activity at JYFL

T. Kalvas\*, O. Tarvainen\*, J. Komppula\*, M. Laitinen\*, T. Sajavaara\*,  
H. Koivisto\*, A. Jokinen\* and M. P. Dehnel†

\**Department of Physics, University of Jyväskylä, P.O. Box 35, 40014, Finland*

†*D-Pace, Inc. P.O. Box 201, Nelson, B.C., Canada V1L 5P9*

**Abstract.** A filament-powered multicusp ion source for production of  $H^-$  has been developed for the Jyväskylä Pelletron accelerator for use in ion beam lithography and particle induced X-ray emission applications. The source can be considered conventional with the exception of the filter field being created with an electric magnet for continuous adjustability. A permanent magnet dipole-antidipole electron dump is integrated in the puller electrode. The source provides  $50 \mu A H^-$  beam at 10 keV energy with 0.019 mm mrad 95 % normalized rms emittance through a 2 mm aperture. Lower emittance is achievable by changing the plasma electrode insert to a smaller aperture one if application requires. A new commercial MCC30/15 cyclotron has been installed at the Jyväskylä accelerator laboratory providing 30 MeV  $H^+$  and 15 MeV  $D^+$  for use in nuclear physics experiments and applications. The ion source delivered with the cyclotron is a filament-powered multicusp source capable of about 130 h continuous operation at 1 mA  $H^-$  output between filament changes. The ion source is located in the cyclotron vault and therefore a significant waiting time for the vault cooldown is required before filament change is possible. This kind of operation is not acceptable as 350 h and longer experiments are expected. Therefore a project for developing a CW 13.56 MHz RF ion source has been initiated. A planar RF antenna replacing the filament back plate of the existing TRIUMF-type ion source has been used in the first tests with 240  $\mu A$  of  $H^-$  and 21 mA of electrons measured at 1.5 kW of RF power. Tests with higher RF power levels were prevented by electron beam induced sparking. A new plasma chamber has been built and a new extraction is being designed for the RF ion source. The extraction code IBSimu has recently gone through a major update on how smooth electrode surfaces are implemented in the Poisson solvers. This has made it possible to implement a fast multigrid solver with low memory consumption. Also a method has been made to import 3D CAD geometries into simulations.

**Keywords:** negative ion source, pelletron, cyclotron, RF, ion optics simulation

**PACS:** 52.50.Dg, 29.25.Ni, 41.75.Cn, 41.85.Ar

## $H^-$ ION SOURCE FOR PELLETRON ACCELERATOR

The 1.7 MV Pelletron accelerator was donated to the Department of Physics, University of Jyväskylä (JYFL) Accelerator Laboratory by VTT Technical Research Center of Finland in 2006 and since then, active development of the Pelletron facility has taken place [1]. The main applications of the Pelletron facility are modification and analysis of materials using ion beam lithography, Rutherford backscattering (RBS), particle induced X-ray emission (PIXE) and time-of-flight elastic recoil detection analysis (ToF-ERDA). In the beginning of 2011 the accelerator was equipped with SNICS and Alphatross ion sources for production of negative ions from  $H^-$  to  $Au^-$ . The PIXE and lithography applications in addition to the planned microbeam imaging facility [2] would benefit significantly from increased  $H^-$  beam brightness and better stability compared to the  $H^-$  beams available from the Alphatross and SNICS ion sources. Therefore a project

was started to develop PELLIS, the *Pelletron Light Ion Source*, an ion source dedicated for high-brightness  $H^-$  beam production.

## Ion Source Design

The PELLIS ion source shown in figure 1 is a filament-driven multicusp ion source with 78 mm plasma chamber diameter. The plasma confinement is achieved with 16  $10 \times 10 \times 120$  mm NdFeB-42 magnets in a multicusp arrangement immersed in cooling water. On the ion source back plate there are 4 rows of  $7 \times 7 \times 77$  mm NdFeB-42 magnets to form a continuation of the cusp. Between the back plate cusps there is a single 1.5 mm diameter tantalum filament, which is heated with a 70–80 A DC current to maintain up to 8 A, 100–120 V arc discharge driving the plasma. The aluminum front plate of the ion source has a 18–10.1 mm diameter, 23.5 mm long conical channel leading to a plasma electrode insert with 2 mm diameter aperture. The insert can be easily changed if higher current or lower emittance beam is required. Inside the front plate there is also a pair of electric magnets creating an adjustable electron filter field aiding the volume production of  $H^-$ . The magnets are wound with 0.95 mm diameter copper wire around SS430 cores with  $3 \times 70$  rounds each. The electric magnets are immersed in cooling water and tolerate up to 20 A of current for a maximum filter field of 67 mT. The ion source filter field is separated from the extraction area by a plasma-electrode insert made from magnetic SS430 steel. The steel insert acts as a field clamp minimizing the penetration of the filter field to the extraction, which would cause unwanted bending of the beam. The plasma meniscus is located in a volume, where  $|B| < 9$  mT with all possible electric magnet settings and  $|B| < 4$  mT with the typical magnet current of less than 2 A. See figure 2 for magnetic field on the ion source axis with different magnet currents.

The ion source extraction is quite similar to the Texas A&M Cyclotron Institute  $H^-$  ion source [4]. A typical injection energy used on the Pelletron accelerator is 10 keV. Therefore the ion source is nominally at  $-10$  kV with respect to the laboratory ground, but voltages from  $-6$  to  $-15$  kV can be used. The puller electrode, which is at fixed  $+6$  kV potential with respect to the ion source, has a dipole-antidipole magnetic field formed by  $40 \times 5 \times 5 \times 5$  mm NdFeB-42 magnets for deflecting the co-extracted electrons into the integrated water-cooled electron dump while the ion beam continues with roughly unaltered angle due to the correcting antidipole-field. This allows a simpler mechanical design compared to the Texas A&M case, where the ion source was tilted to compensate the ion beam deflection in the magnetic field. The magnetic puller electrode is followed by an einzel electrode with a nominal  $-6$  kV potential, which is used to optimize the beam transmission to the accelerator. The last electrode is at ground. The ion beam suffers from a slight offset inside the puller electrode due to the electron dump magnetic field. This causes the beam to bend to a 5 mrad angle in the einzel lens. Nevertheless, the simulated rms emittance of the ion beam at the end of the extraction ( $z = 100$  mm in figure 3) is between 0.017 and 0.02 mm mrad in the cases where the puller-electrode voltage is optimized for the plasma density. This is very low as the theoretical minimum emittance for 1 eV transverse ion temperature used in the simulations is 0.016 mm mrad. See figures 3 and 4 for an example of a 3D extraction simulations, made with IBSimu [4].

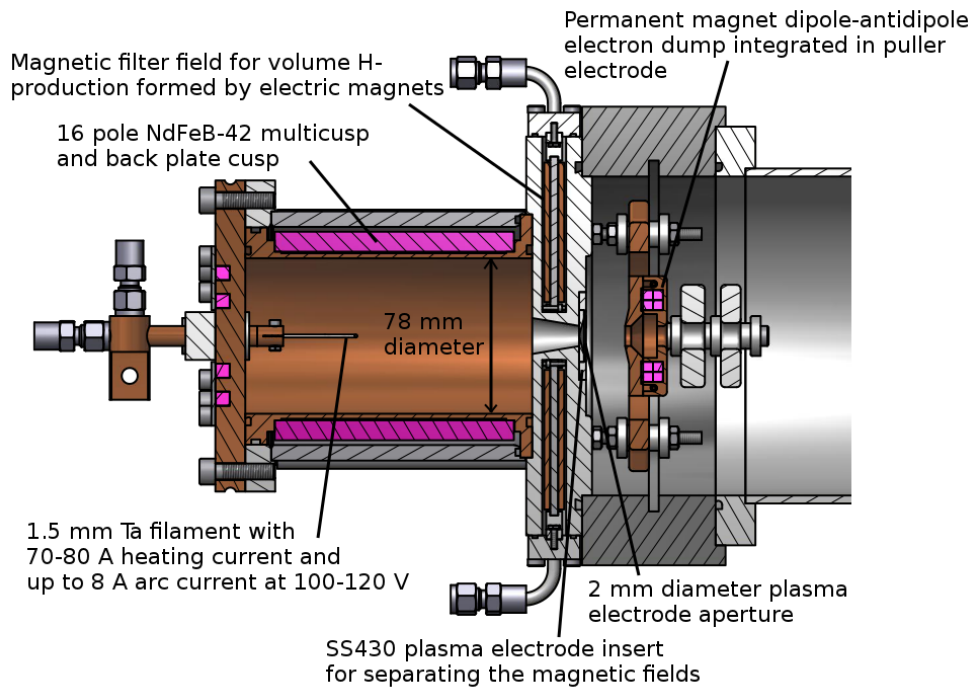


**FIGURE 1.** Cross-sectional view of the PELLIS ion source with main parts labelled.

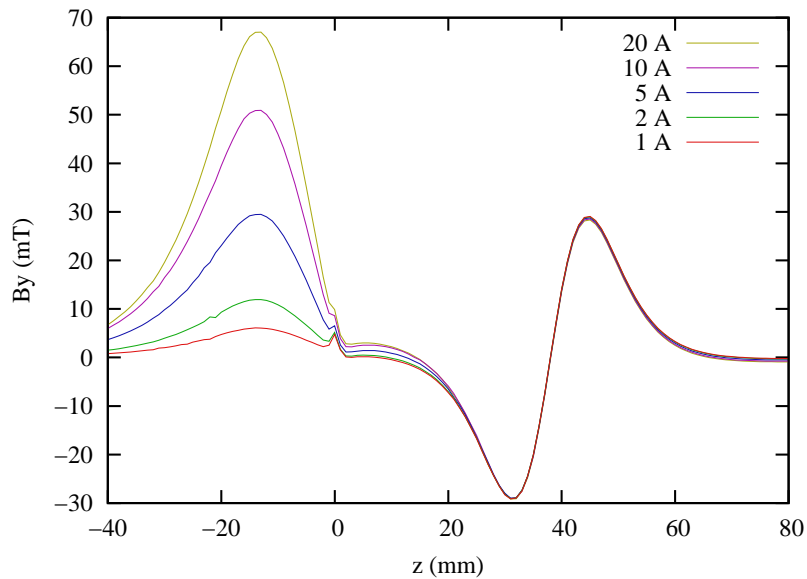


**FIGURE 2.** Magnetic field  $B_y$  simulated with Radia-3D [3] on the ion source axis with different currents on the electric magnet. The origin ( $z = 0$ ) is at the plasma electrode surface facing the plasma and positive  $z$ -direction is towards the extraction. The other magnetic field components are zero on the axis.

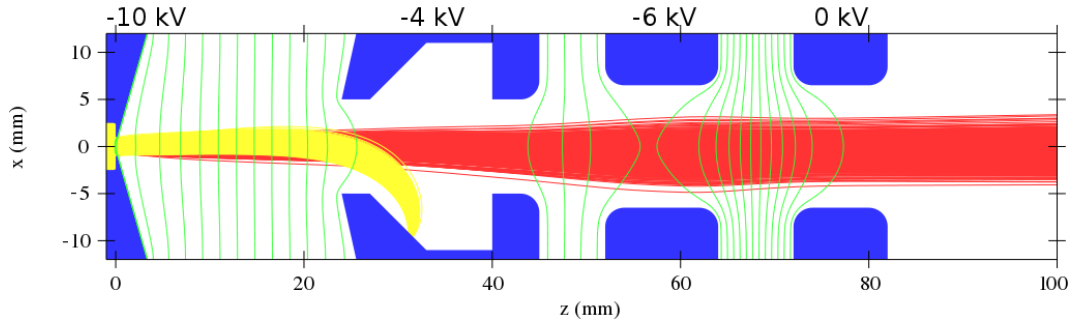


**FIGURE 3.** Three-dimensional simulation of the PELLIS extraction with 3.5 mA electron beam (yellow) being deflected into the electron dump and 100  $\mu\text{A}$   $\text{H}^-$  beam (red) continuing through the extraction.

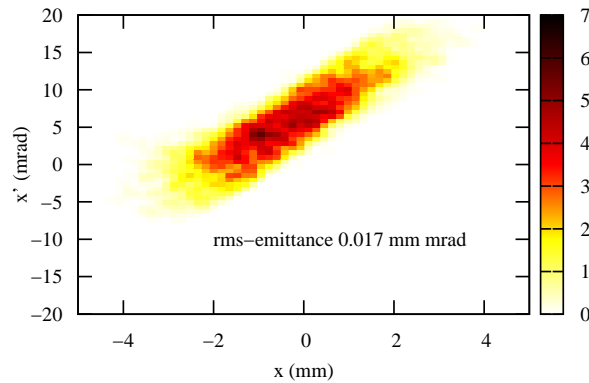


**FIGURE 4.** Emittance plot at  $z = 100$  mm from the simulation shown in figure 3.

The ion source and the extraction vacuum chamber with a second einzel lens are installed in the middle branch of the three-way switching magnet of the accelerator injection line at a 2 degree angle. The angle is small enough to allow optical alignment of the accelerator through the extraction vacuum chamber. On the other hand it is large enough to prevent fast neutrals, born via beam stripping in the high background gas pressure areas of the extraction, from entering the accelerator. The switching magnet is used together with following electrostatic deflector plates to correct for 2 degree bend at the magnet and the effects of the 5 mrad angular error at the first einzel lens.

## Measurements

The ion source was installed in February 2012 and it was characterized with current and emittance measurements. The  $\text{H}^-$  current was determined using a Faraday cup at 195 mm from the plasma electrode and the  $\text{e}^-$  current was determined from the puller high voltage power supply drain. The beam currents were measured as a function of the arc current and filter magnetic field at constant 0.5 Pa ion source pressure, which is the optimum pressure for  $\text{H}^-$  production at 1 A arc current. The measurement results are shown in figure 5.

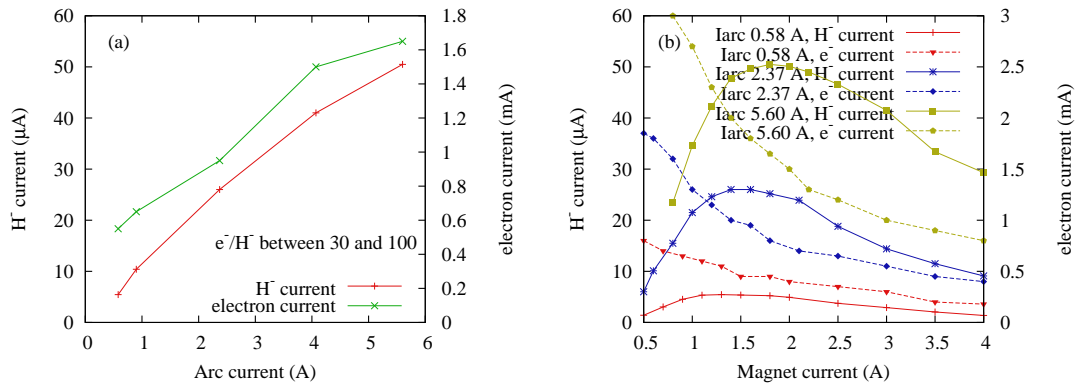


**FIGURE 5.** (a) The H<sup>-</sup> and electron currents as a function of arc current with filter field optimized for maximal ion production. (b) Ion and electron currents as a function of filter magnet current for different arc currents. Filter field dependence on magnet current can be seen in figure 2.

The current measurements show that the optimum filter field does not change strongly with plasma density: between 0.58 and 5.6 A arc currents the optimum filter peak field is between 8 and 11 mT correspondingly. The effect of ion source pressure to the optimum filter field is still to be studied as results from a TRIUMF-type H<sup>-</sup> source at JYFL suggest that varying neutral gas pressure changes electron dynamics drastically [5]. The extracted ion current is not very sensitive to the filter field strength and therefore for future ion sources of this type the filter field could be made with permanent magnets optimized by trying different magnet grades or sizes, compromising 5–10 % of the performance. On the other hand, on state-of-the-art volume production ion sources, changing from permanent magnet filter to an electric magnet to achieve a small gain in performance may be worth the increased complexity.

For the emittance measurements, an Allison-type scanner was attached to the ion source main insulator with its first collimator at 169 mm from the plasma electrode. Emittance measurements were made with different arc currents and different puller electrode voltages. The emittance data was filtered by thresholding to contain 95 % of the beam. The results are shown in figure 6. The measured emittance values are of about the same magnitude as the simulated ones with transverse temperature of 1 eV, but it seems that the extraction is not operating optimally at these currents. The emittance values are decreasing as extracted H<sup>-</sup> current increases. The extraction was designed for 100 μA beam current with 6 kV gap voltage. Assuming that the simulations are correct the extraction should be changed by increasing the plasma electrode-puller gap to reach the minimum emittance at the typical beam intensities of 15–30 μA. Additional experiments have already been planned to first measure emittance at higher beam intensities and again after increasing the plasma electrode-puller gap.

## ION SOURCE FOR MCC30/15 CYCLOTRON

An agreement was made in 2006 between Finland and Russia to settle the former debt of USSR to Finland by goods and services. The two countries negotiated that as part

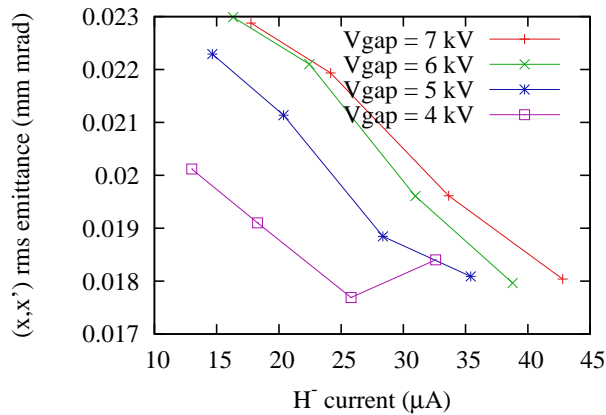


**FIGURE 6.** The rms emittances measured from the ion source using different acceleration voltages in the first plasma electrode-puller gap.

of the debt, a MCC30/15 cyclotron was to be manufactured and installed at JYFL by the D. V. Efremov Institute, St. Petersburg, Russia. The device was delivered in August 2009 and approved for use in April 2010. The cyclotron produces up to 200  $\mu\text{A}$  of 18–30 MeV  $\text{H}^+$  and up to 60  $\mu\text{A}$  of 9–15 MeV  $\text{D}^+$  from negative ions with high-efficiency stripping extraction. The beams will be used for medical isotope production and nuclear physics experiments at the IGISOL facility. [6]

The ion source delivered with the cyclotron is a conventional filament-driven multicusp source for production of  $\text{H}^-$  and  $\text{D}^-$ . The ion source is capable of continuous operation at 1 mA  $\text{H}^-$  output for about 130 hours before filament failure. The ion source is located at 2.1 m from the accelerator within the cyclotron vault. The filament renewal can take about 12 hours because of the required vault cooldown before access to ion source is possible. This kind of operation is not acceptable as 350 h and longer continuous experiments are expected once the facility is fully operational. Therefore a project for developing a CW 13.56 MHz *Radiofrequency Ion Source*, RADIS, for the cyclotron was initiated in March 2011. The goal of the RADIS project is to develop a new ion source to produce at least 1 mA of CW  $\text{H}^-$  beam or 500  $\mu\text{A}$  of CW  $\text{D}^-$  beam at the cyclotron injection energy of 19 keV, with a maintenance interval of at least one month.

The first design being studied for the RADIS is a multicusp chamber with an external planar spiral RF antenna behind a flat AlN RF window on the back of the ion source. A similar approach has been studied at Seoul National University (SNU) with promising results [7]. The studies have been started by using the TRIUMF-type  $\text{H}^-$  ion source LIISA as a retrofitted test stand. Normally the source is used to inject  $\text{H}^-$  at 5.9 keV injection energy to the laboratory K130 cyclotron [8]. The test stand beam energy is much lower than the design goal of RADIS, but it is sufficient for testing purposes. The ion source filament back plate has been replaced with a new RF back plate for the tests as shown in figure 7. The water-cooled flat RF antenna of the source is made from 6.35 mm diameter copper tubing and the antenna rounds are insulated from each other with 0.2 mm thick shrink tubing. The 5 kW CW RF power supply is coupled to the antenna using a capacitive T network matching circuit. The RF power supply, matching network

and the antenna are all at high voltage.

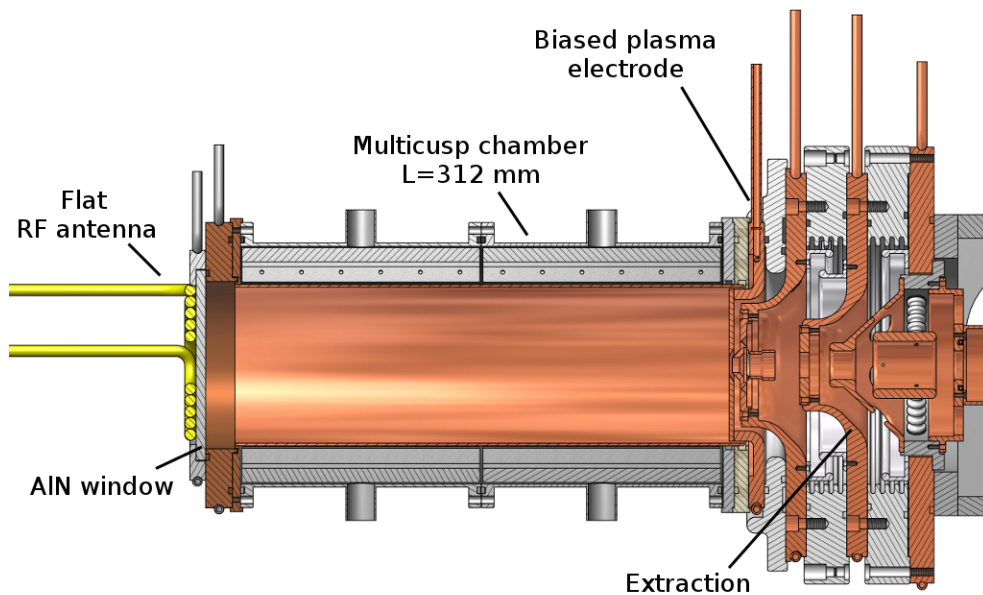


**FIGURE 7.** Cross-sectional view of the setup used for RF ion source testing.

So far the experiments on the test source have not produced as much data as has been expected because operating the ion source, especially at RF power levels higher than 1 kW, causes faults in the central control system. It is suspected that this is due to high voltage sparking in the extraction, induced by higher co-extracted electron currents compared to filament-driven operation ( $e^-/H^-$  ratio has been about 100 in measurements while for typical run with filament back-plate the ratio is about 5). Because of incorrect grounding scheme at the ion source the high-voltage sparks cause variations in the control system ground level inducing false control signals in the system. The best results with the test source have been 240  $\mu A$  of  $H^-$  and 21 mA of electrons at 1500 W RF input (307 W reflected) with 15 V plasma-electrode bias and optimized pressure. To achieve higher ion beam current, the grounding circuits of the retrofitted test stand have to be reconstructed.

The test ion source has a 312 mm long plasma chamber. It is expected that a higher power efficiency can be achieved with a shorter chamber when the plasma is driven with an RF discharge. A new 127 mm long aluminum Modified MultiPole Structure (MMPS) [9] multicusp chamber, compatible with the existing RF back plate, has been built for RADIS. The chamber is shown in figure 8. The MMPS configuration of the chamber uses magnetic SS430 steel strips to redirect the magnetic flux at the poles. The biggest plasma losses are at the magnetic poles and therefore the heat flow to the permanent magnets is smaller in MMPS compared to a conventional multicusp configuration, where magnets are located at the poles. The new chamber is going to be attached to a PELLIS-style front plate with an electric magnet filter field. The front plate is going to be electrically insulated from the plasma chamber to enable plasma-electrode biasing. Also a new extraction system, which is capable of handling up to 100 mA of co-extracted electron current is being designed to be used with this chamber. The

extraction uses a similar electron dumping scheme what has been planned to be used at CERN Linac4 and at Spallation Neutron Source (SNS) [10, 11]. The new extraction is going to have an adjustable voltage on puller electrode for experimental matching to the plasma density for optimum beam quality. The electron dumping will be performed on the following decelerating einzel lens at about 6 keV energy leading to about 600 W of heat being dumped on the electrode, which is the biggest engineering challenge on the extraction. The einzel lens is followed by a grounded electrode and another accelerating einzel lens for adjusting the beam focusing and for enabling space charge compensation in the following beam line. Preliminary extraction simulations are shown in figure 9.

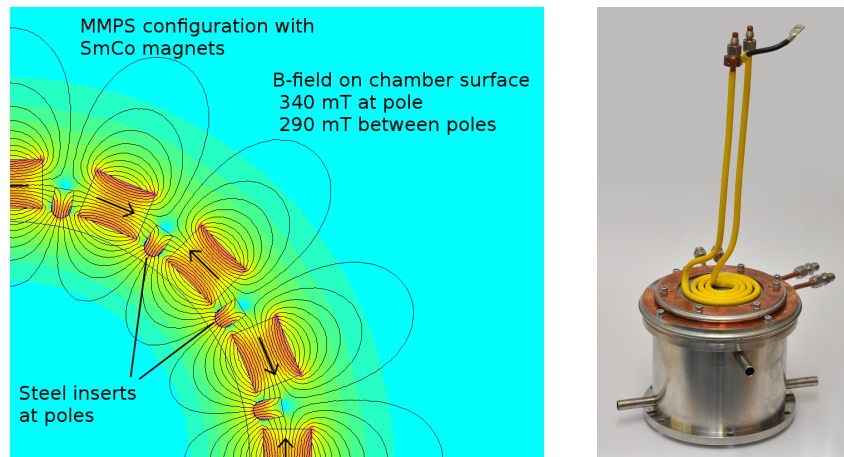


**FIGURE 8.** FEMM simulation image of the SmCo MMPS multicusp configuration on the left and photograph of the finished chamber with the RF back plate on the right.

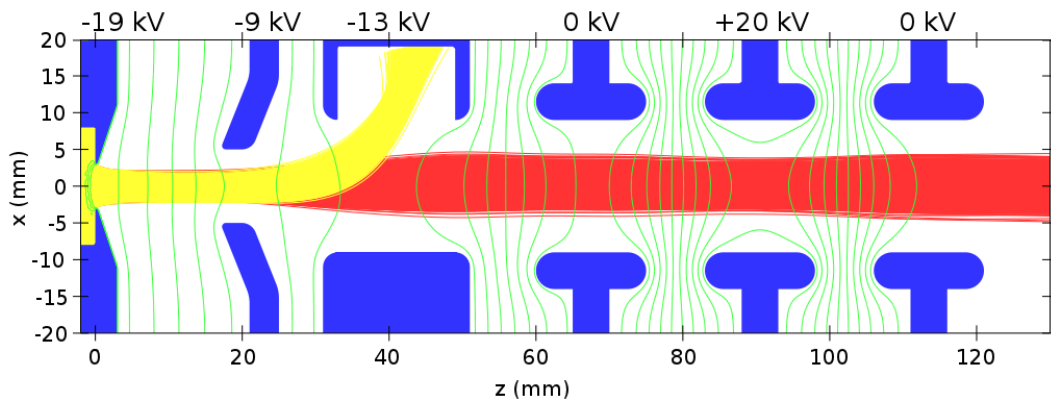


**FIGURE 9.** Three-dimensional simulation with 1 mA of  $H^-$  and 100 mA of electrons being extracted with the preliminary extraction design for RADIS.

The ion source design allows testing other concepts as well. One of the approaches that have been planned is the use of an RF plasma cathode similarly as in reference [12]: A spiral RF antenna can be used to excite a high-density small-volume plasma, from which an electron beam is pulled at low energy using a triode grid to drive the main discharge in a larger multicusp chamber. The triode grid voltages can be optimized for volume production of  $H^-$  in the main chamber, while preventing positive ions from entering the cathode. This kind of setup would allow similar plasma conditions

to filament-driven ion sources with primary electron energies of about 100 eV, which has been proven suitable for cesium-free CW  $H^-$  ion sources, but without the lifetime limitation of thermionic filaments. This kind of arrangement is expected to increase the power efficiency compared to directly heated RF ion source.

The RADIS ion source is also going to be a tool for studying the UV-light assisted production of  $H^-$  on negative electron affinity surfaces [13, 5]. The RF ion source provides a plasma discharge relatively free of surface coating and therefore it is suitable for such an experiment.

## RECENT UPDATES ON IBSIMU EXTRACTION CODE

The extraction code IBSimu [4] has recently gone through a major update on how smooth electrode surfaces are implemented in the Poisson solvers. The old method used virtual potential nodes inside the electrodes. These nodes caused low field accuracy and convergence problems in certain cases. The new method uses modified finite difference Poisson equation with unequal node distances at nodes, which are at less than one mesh distance  $h$  from electrode surfaces. The modified Poisson is

$$\frac{\beta\phi(x_0 - \alpha h) - (\alpha + \beta)\phi(x_0) + \alpha\phi(x_0 + \beta h)}{\frac{1}{2}(\alpha + \beta)\alpha\beta h^2} = -\frac{\rho(x_0)}{\epsilon_0} \quad (1)$$

where  $\phi$  is potential,  $h$  is the nominal mesh spacing and  $\alpha$  and  $\beta$  are relative distances to neighbouring nodes (or surfaces) as shown in figure 10. The surface-to-node distances  $\alpha$  and  $\beta$  are saved to a database for this purpose. Also the calculation of electric fields from the potential data takes in account the modified distances. The new method has superior accuracy close to electrode surfaces compared to the old method. It has also made it possible to implement a multigrid solver in IBSimu for fast and low memory consumption calculations of large problems.

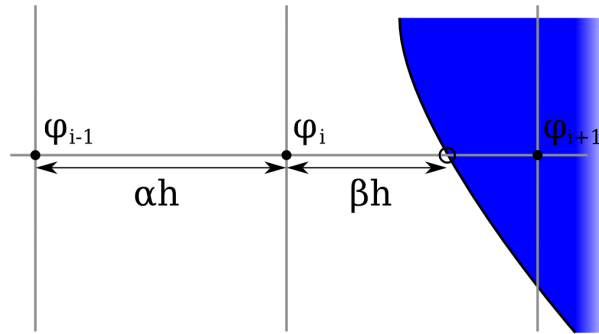


**FIGURE 10.** Example of calculation node distances in one dimension. The effective distance from node  $i$  to node  $i+1$  is less than  $h$  due to the electrode (blue) surface. The distance is  $\beta h$ , where  $0 < \beta < 1$ . In the example shown  $\alpha = 1$ .

A method has been added in IBSimu to import 3D CAD geometries into simulations using triangulated surface representation in STL file format. This makes it possible to easily simulate systems with complicated electrode geometries. Also an option has been added for relativistic particle trajectory calculation.

## ACKNOWLEDGMENTS

This work has been supported by the EU 7th framework programme “Integrating Activities - Transnational Access”, project number: 262010 (ENSAR) and by the Academy of Finland under the Finnish Centre of Excellence Programme 2006–2011 (Nuclear and Accelerator Based Physics Research at JYFL).

## REFERENCES

1. M. Laitinen, J. Julin, L. Mättö, M. Napari, N. Puttaraksa and T. Sajavaara, in these proceedings.
2. R. Norarat, T. Sajavaara, M. Laitinen, P. Heikkinen, K. Ranttila, K. Ylikorkala, V. Hänninen, M. Rossi, P. Jones, V. Marjomäki, L. Gilbert and H. J. Whitlow, *Nucl. Instrum. Meth. B* **272**, 158 (2012).
3. O. Chubar, P. Elleaume and J. Chavanne, *Radia3D — A computer program for calculating static magnetic fields*, <http://www.esrf.eu/Accelerators/Groups/InsertionDevices/Software/Radia> (2012)
4. T. Kalvas, O. Tarvainen, T. Ropponen, O. Steczkiewicz, J. Ärje, and H. Clark, *Rev. Sci. Instrum.* **81**, 02B703 (2010).
5. J. Komppula, S. Lähti, O. Tarvainen, T. Kalvas, H. Koivisto, V. Toivanen and P. Myllyperkiö, in these proceedings.
6. P. Heikkinen, *Proc. of the 19th International Conference on Cyclotrons and their Applications*, September 6-10, 2010, Lanzhou, China, p. 310-312 (<http://www.jacow.org/>)
7. Y. An, W. H. Cho, K-J Chung, K. Lee, S. B. Jang, S. G. Lee and Y. S. Hwang, *Rev. Sci. Instrum.* **83**, 02A727 (2012).
8. T. Kuo, R. Baartman, G. Dutto, S. Hahto, J. Ärje, and E. Liukkonen, *Rev. Sci. Instrum.* **73**, 986 (2002).
9. H. Koivisto, P. Suominen, O. Tarvainen and D. Hitz, *Rev. Sci. Instrum.* **75**, 1479 (2004).
10. Ø. Midttun, T. Kalvas, M. Kronberger, J. Lettry, H. Pereira and R. Scrivens, in these proceedings.
11. T. Kalvas, R. F. Welton, O. Tarvainen, B. X. Han, and M. P. Stockli, *Rev. Sci. Instrum.* **83**, 02A705 (2012).
12. R. Keller, P. Luft, M. Regis, J. Wallig, M. Monroy, A. Ratti, D. Syversrud, R. Welton and D. Anderson, *Proc. of 2005 Particle Accelerator Conference*, Knoxville, Tennessee, 1784 (2005).
13. O. Tarvainen, T. Kalvas, J. Komppula, H. Koivisto, E. Geros, J. Stelzer, G. Rouleau, K. F. Johnson and J. Carmichael, *AIP Conf. Proc.* **1390**, 113 (2011).